J|A|C|S
ARTICLES

Published on Web 05/15/2009

Photoinduced Charge Transfer and Electrochemical Properties of Triphenylamine I_h-$Sc_3N@C_{80}$ Donor−Acceptor Conjugates

Julio R. Pinzón,[†] Diana C. Gasca,[†] Shankara G. Sankaranarayanan,[§] Giovanni Bottari,[‡] Tomás Torres,[‡] Dirk M. Guldi,[§] and Luis Echegoyen*[,†]

Department of Chemistry, Clemson University, Clemson, South Carolina 29634, Department of Chemistry and Pharmacy and Interdisciplinary Center for Molecular Materials (ICMM), Friedrich-Alexander-Universität Erlangen-Nürnberg, Egerlandstrasse 3, 91058 Erlangen, Germany, and Departamento de Química Orgánica, Universidad Autónoma de Madrid, E-28049 Madrid, Spain

Received January 29, 2009; E-mail: luis@clemson.edu

Abstract: Two isomeric [5,6]-pyrrolidine−I_h-$Sc_3N@C_{80}$ electron donor−acceptor conjugates containing triphenylamine (TPA) as the donor system were synthesized. Electrochemical and photophysical studies of the novel conjugates were made and compared with those of their C_{60} analogues, in order to determine (i) the effect of the linkage position (*N*-substituted versus 2-substituted pyrrolidine) of the donor system in the formation of photoinduced charge separated states, (ii) the thermal stability toward the retro-cycloaddition reaction, and (iii) the effect of changing C_{60} for I_h-$Sc_3N@C_{80}$ as the electron acceptor. It was found that when the donor is connected to the pyrrolidine nitrogen atom, the resulting dyad produces a significantly longer lived radical pair than the corresponding 2-substituted isomer for both the C_{60} and I_h-$Sc_3N@C_{80}$ dyads. In addition to that, the *N*-substituted TPA−I_h-$Sc_3N@C_{80}$ dyad has much better thermal stability than the 2-subtituted one. Finally, the I_h-$Sc_3N@C_{80}$ dyads have considerably longer lived charge separated states than their C_{60} analogues, thus approving the advantage of using I_h-$Sc_3N@C_{80}$ instead of C_{60} as the acceptor for the construction of fullerene based donor−acceptor conjugates. These findings are important for the design and future application of I_h-$Sc_3N@C_{80}$ dyads as materials for the construction of plastic organic solar cells.

Introduction

Fullerenes have been proposed as acceptor materials in the construction of plastic solar cell devices due to their unique structural and electron acceptor characteristics.[1] Most of the fullerene-based solar cells are made using the bulk heterojunction concept, where a conjugated polymer acting as a donor is blended with a fullerene derivative with improved solubility acting as the acceptor.[2] The maximum power conversion efficiencies with this type of cells have recently reached 5.5%.[3] Hence higher efficiencies seem to be feasible, both theoretically and in practice.[4] The molecular heterojunction concept where a donor molecule is covalently connected to a fullerene is one of the possible alternatives to further improve the efficiency of plastic fullerene-based solar cells.[5] Since organic molecules allow a high degree of structural control; fine-tuning of the charge separation properties, charge mobility and spatial orientation of the donor group relative to the acceptor can be achieved by using specifically engineered molecular systems.[6] Following this principle, donor−acceptor conjugates with the ability to efficiently generate long-lived charge separated states with lifetimes comparable to the ones observed in natural photosynthetic systems have been synthesized.[7]

Among the large number of fullerenes that have the potential to replace C_{60} or C_{70} as optimal electron acceptors in fullerene-

[†] Clemson University.
[§] Friedrich-Alexander-Universität Erlangen-Nürnberg.
[‡] Universidad Autónoma de Madrid.

(1) (a) Thompson, B. C.; Frechet, J. M. J. *Angew. Chem., Int. Ed.* **2008**, *47*, 58–77. (b) Araki, Y.; Ito, O. *J. Photochem. Photobiol., C.* **2008**, *9*, 93–110. (c) Imahori, H. *Bull. Chem. Soc. Jpn.* **2007**, *80*, 621–636. (d) Guenes, S.; Neugebauer, H.; Sariciftci, N. S. *Chem. Rev.* **2007**, *107*, 1324–1338. (e) Blom, P. W. M.; Mihailetchi, V. D.; Koster, L. J. A.; Markov, D. E. *Adv. Mater.* **2007**, *19*, 1551–1566. (f) Koeppe, R.; Sariciftci, N. S. *Photochem. Photobiol. Sci.* **2006**, *5*, 1122–1131.
(2) Yu, G.; Gao, J.; Hummelen, J. C.; Wudl, F.; Heeger, A. J. *Science* **1995**, *270*, 1789–1791.
(3) (a) Lee, J. K.; Ma, W. L.; Brabec, C. J.; Yuen, J.; Moon, J. S.; Kim, J. Y.; Lee, K.; Bazan, G. C.; Heeger, A. J. *J. Am. Chem. Soc.* **2008**, *130*, 3619–3623. (b) Peet, J.; Kim, J. Y.; Coates, N. E.; Ma, W. L.; Moses, D.; Heeger, A. J.; Bazan, G. C. *Nat. Mater.* **2007**, *6*, 497–500. (c) Kim, J. Y.; Lee, K.; Coates, N. E.; Moses, D.; Nguyen, T.; Dante, M.; Heeger, A. J. *Science* **2007**, *317*, 222–225.
(4) (a) Dennler, G.; Scharber, M. C.; Ameri, T.; Denk, P.; Forberich, K.; Waldauf, C.; Brabec, C. J. *Adv. Mater.* **2008**, *20*, 579–583. (b) Muehlbacher, D.; Scharber, M.; Morana, M.; Zhu, Z.; Waller, D.; Gaudiana, R.; Brabec, C. *Adv. Mater.* **2006**, *18*, 2884–2889.
(5) (a) Roncali, J. *Chem. Soc. Rev.* **2005**, *34*, 483–495. (b) Segura, J. L.; Martin, N.; Guldi, D. M. *Chem. Soc. Rev.* **2005**, *34*, 31–47.
(6) (a) Fukuzumi, S. *Phys. Chem. Chem. Phys.* **2008**, *10*, 2283–2297. (b) Fukuzumi, S.; Kojima, T. *J. Mater. Chem.* **2008**, *18*, 1427–1439. (c) Martin, N.; Sanchez, L.; Herranz, M. A.; Illescas, B.; Guldi, D. M. *Acc. Chem. Res.* **2007**, *40*, 1015–1024.
(7) (a) Guldi, D. M.; Imahori, H.; Tamaki, K.; Kashiwagi, Y.; Yamada, H.; Sakata, Y.; Fukuzumi, S. *J. Phys. Chem. A* **2004**, *108*, 541–548. (b) Imahori, H.; Sekiguchi, Y.; Kashiwagi, Y.; Sato, T.; Araki, Y.; Ito, O.; Yamada, H.; Fukuzumi, S. *Chem.—Eur. J.* **2004**, *10*, 3184–3196.

based solar cells, I_h-$Sc_3N@C_{80}$, which was discovered a few years ago by Dorn and co-workers,[8] is very attractive due to its outstanding ability to stabilize charge-separated states when compared to C_{60}, as shown in our previous study.[9] Recent developments have allowed its preparation[10] and isomeric separation in bulk quantities by non-HPLC methods[11] with a higher yield than C_{84}, the third most abundant empty fullerene.[12] Due to its high symmetry, I_h-$Sc_3N@C_{80}$ has only two types of double bonds, described as [5,6] when they are between five- and a six-membered rings and [6,6] when they are between two six-membered rings. These bonds have different reactivity and yield derivatives with different electrochemical behavior.[13] On the other hand, triphenylamine (TPA) and its derivatives are robust molecules that have been successfully employed as donors for the construction of small-molecule donor solution processable organic solar cells,[14] dye-sensitized solar cells,[15] and fullerene donor−acceptor conjugates[16] because of their strong donor character, their good hole transport properties,[17] their propeller structure which benefits the solution processability,[14a] and their ability to form and stabilize radical cations.[17b]

1,3-Dipolar cycloaddition of azomethine ylides to fullerenes is a common strategy for the functionalization of fullerenes.[18] However, there are very few examples of fulleropyrrolidine donor−acceptor conjugates where the donor group is connected to the nitrogen atom of the pyrrolidine ring.[19] Other examples of donor groups connected axially using the nitrogen atom in the pyrrolidine ring are coordinated compounds using a fullerene derivative as a ligand[20] or supramolecular assemblies;[21] however, attaching the donor groups to the 2-position of the pyrrolidine ring is usually the preferred choice. In our previous studies[9b] it was also observed that the 2-substituted I_h-$Sc_3N@C_{80}$ and I_h-$Y_3N@C_{80}$ pyrrolidine derivatives can undergo thermal 1,3-retrocycloaddition reactions.[22] Importantly, there are no reports of systematic studies comparing the stability of *N*-substituted fulleropyrrolidines versus 2-substituted analogues and the effect of the substitution pattern on the efficiency of the charge separation process and/or thermal stability. To address these questions, we have prepared two isomeric TPA−I_h-$Sc_3N@C_{80}$ fulleropyrrolidine electron donor−acceptor conjugates and compared their properties with those of the corresponding C_{60} conjugates in order to study the effect of the pyrrolidine linkage position and the effect of changing the fullerene acceptor on the efficiency of the charge separation process.

Results and Discussion

Synthesis of Electron Donor−Acceptor Conjugates. To date, the reported chemical reactions on the I_h-$Sc_3N@C_{80}$ cage include Diels−Alder,[23] hydroxylation,[24] 1,3-dipolar cycloaddition of azomethine ylides,[9,13,25] disilirane addition,[26] radical trifluoromethylation,[27] malonate-free radical addition,[28] and dibenzyl-

(8) Stevenson, S.; Rice, G.; Glass, T.; Harlch, K.; Cromer, F.; Jordan, M. R.; Craft, J.; Hadju, E.; Bible, R.; Olmstead, M. M.; Maltra, K.; Fisher, A. J.; Balch, A. L.; Dorn, H. C. *Nature* **1999**, *401*, 55–57.

(9) (a) Pinzón, J. R.; Plonska-Brzezinska, M. E.; Cardona, C. M.; Athans, A. J.; Gayathri, S. S.; Guldi, D. M.; Herranz, M. A.; Martin, N.; Torres, T.; Echegoyen, L. *Angew. Chem., Int. Ed.* **2008**, *47*, 4173–4176. (b) Pinzón, J. R.; Cardona, C. M.; Herranz, M. A.; Plonska-Brzezinska, M. E.; Palkar, A.; Athans, A. J.; Martín, N.; Rodríguez-Fortea, A.; Poblet, J. M.; Bottari, G.; Torres, T.; Gayathri, S. S.; Guldi, D. M.; Echegoyen, L. *Chem.−Eur. J.* **2009**, *15*, 864–877.

(10) (a) Stevenson, S.; Mackey, M. A.; Thompson, M. C.; Coumbe, H. L.; Madasu, P. K.; Coumbe, C. E.; Phillips, J. P. *Chem. Commun.* **2007**, *41*, 4263–4265. (b) Stevenson, S.; Thompson, M. C.; Coumbe, H. L.; Mackey, M. A.; Coumbe, C. E.; Phillips, J. P. *J. Am. Chem. Soc.* **2007**, *129*, 16257–16262.

(11) (a) Angeli, C. D.; Cai, T.; Duchamp, J. C.; Reid, J. E.; Singer, E. S.; Gibson, H. W.; Dorn, H. C. *Chem. Mater.* **2008**, *20*, 4993–4997. (b) Stevenson, S.; Mackey, M. A.; Coumbe, C. E.; Phillips, J. P.; Elliott, B.; Echegoyen, L. *J. Am. Chem. Soc.* **2007**, *129*, 6072–6073. (c) Stevenson, S.; Yu, H.; Carpenter, K.; Heaps, D. T.; Stephen, R.; Coumbe, C.; Harich, K.; Phillips, J. P. *ECS Trans.* **2007**, *2*, 95–102. (d) Stevenson, S.; Harich, K.; Yu, H.; Stephen, R. R.; Heaps, D.; Coumbe, C.; Phillips, J. P. *J. Am. Chem. Soc.* **2006**, *128*, 8829–8835. (e) Ge, Z.; Duchamp, J. C.; Cai, T.; Gibson, H. W.; Dorn, H. C. *J. Am. Chem. Soc.* **2005**, *127*, 16292–16298. (f) Elliott, B.; Yu, L.; Echegoyen, L. *J. Am. Chem. Soc.* **2005**, *127*, 10885–10888.

(12) Kratschmer, W.; Lamb, L. D.; Fostiropoulos, K.; Huffman, D. R. *Nature* **1990**, *347*, 354–358.

(13) Cardona, C. M.; Elliott, B.; Echegoyen, L. *J. Am. Chem. Soc.* **2006**, *128*, 6480–6485.

(14) For recent examples see: (a) Wu, G.; Zhao, G.; He, C.; Zhang, J.; He, Q.; Chen, X.; Li, Y. *Sol. Energy Mater. Sol. Cells* **2009**, *93*, 108–113. (b) Aleveque, O.; Leriche, P.; Cocherel, N.; Frere, P.; Cravino, A.; Roncali, J. *Sol. Energy Mater. Sol. Cells* **2008**, *92*, 1170–1174. (c) He, C.; He, Q.; Yang, X.; Wu, G.; Yang, C.; Bai, F.; Shuai, Z.; Wang, L.; Li, Y. *J. Phys. Chem. C* **2007**, *111*, 8661–8666. (d) Roquet, S.; Cravino, A.; Leriche, P.; Aleveque, O.; Frere, P.; Roncali, J. *J. Am. Chem. Soc.* **2006**, *128*, 3459–3466.

(15) For recent examples of TPA dye sensitized solar cells: (a) Ma, X.; Hua, J.; Wu, W.; Jin, Y.; Meng, F.; Zhan, W.; Tian, H. *Tetrahedron* **2008**, *64*, 345–350. (b) Qin, P.; Zhu, H.; Edvinsson, T.; Boschloo, G.; Hagfeldt, A.; Sun, L. *J. Am. Chem. Soc.* **2008**, *130*, 8570–8571. (c) Li, G.; Jiang, K.; Li, Y.; Li, S.; Yang, L. *J. Phys. Chem. C* **2008**, *112*, 11591–11599. (d) Xu, W.; Peng, B.; Chen, J.; Liang, M.; Cai, F. *J. Phys. Chem. C* **2008**, *112*, 874–880. (e) Ning, Z.; Zhang, Q.; Wu, W.; Pei, H.; Liu, B.; Tian, H. *J. Org. Chem.* **2008**, *73*, 3791–3797. (f) Liang, M.; Xu, W.; Cai, F.; Chen, P.; Peng, B.; Chen, J.; Li, Z. *J. Phys. Chem. C* **2007**, *111*, 4465–4472.

(16) (a) El-Khouly, M. E.; Shim, S. H.; Araki, Y.; Ito, O.; Kay, K. *J. Phys. Chem. B* **2008**, *112*, 3910–3917. (b) Chen, Y.; El-Khouly, M. E.; Zhuang, X.; He, N.; Araki, Y.; Lin, Y.; Ito, O. *Chem.−Eur. J.* **2007**, *13*, 1709–1714. (c) D'Souza, F.; Gadde, S.; Islam, D. S.; Wijesinghe, C. A.; Schumacher, A. L.; Zandler, M. E.; Araki, Y.; Ito, O. *J. Phys. Chem. A* **2007**, *111*, 8552–8560. (d) El-Khouly, M. E.; Kim, J. H.; Kwak, M.; Choi, C. S.; Ito, O.; Kay, K. *Bull. Chem. Soc. Jpn.* **2007**, *80*, 2465–2472. (e) Sandanayaka, A. S. D.; Taguri, Y.; Araki, Y.; Ishii, T.; Mataka, S.; Ito, O. *J. Phys. Chem. B* **2005**, *109*, 22502–22512. (f) Zeng, H.; Wang, T.; Sandanayaka, A. S. D.; Araki, Y.; Ito, O. *J. Phys. Chem. A* **2005**, *109*, 4713–4720.

(17) (a) Yeh, S. J.; Tsai, C. Y.; Huang, C.; Liou, G.; Cheng, S. *Electrochem. Commun.* **2003**, *5*, 373–377. (b) Tsujii, Y.; Tsuchida, A.; Yamamoto, M.; Nishijima, Y. *Macromolecules* **1988**, *21*, 665–670.

(18) (a) Tagmatarchis, N.; Prato, M. *Synlett* **2003**, 768–779. (b) Maggini, M.; Scorrano, G.; Prato, M. *J. Am. Chem. Soc.* **1993**, *115*, 9798–9799.

(19) (a) Campidelli, S.; Vazquez, E.; Milic, D.; Prato, M.; Barbera, J.; Guldi, D. M.; Marcaccio, M.; Paolucci, D.; Paolucci, F.; Deschenaux, R. *J. Mater. Chem.* **2004**, *14*, 1266–1272. (b) Guldi, D. M.; Luo, C.; Kotov, N. A.; Da Ros, T.; Bosi, S.; Prato, M. *J. Phys. Chem. B* **2003**, *107*, 7293–7298.

(20) (a) Zhou, Z.; Sarova, G. H.; Zhang, S.; Ou, Z.; Tat, F. T.; Kadish, K. M.; Echegoyen, L.; Guldi, D. M.; Schuster, D. I.; Wilson, S. R. *Chem.−Eur. J.* **2006**, *12*, 4241–4248. (b) Galili, T.; Regev, A.; Berg, A.; Levanon, H.; Schuster, D. I.; Moebius, K.; Savitsky, A. *J. Phys. Chem. A* **2005**, *109*, 8451–8458. (c) Tat, F. T.; Zhou, Z.; MacMahon, S.; Song, F.; Rheingold, A. L.; Echegoyen, L.; Schuster, D. I.; Wilson, S. R. *J. Org. Chem.* **2004**, *69*, 4602–4606. (d) Wilson, S. R.; MacMahon, S.; Tat, F. T.; Jarowski, P. D.; Schuster, D. I. *Chem. Commun.* **2003**, 226–227. (e) Guldi, D. M.; Da Ros, T.; Braiuca, P.; Prato, M. *Photochem. Photobiol. Sci.* **2003**, *2*, 1067–1073.

(21) (a) Kuramochi, Y.; Satake, A.; Itou, M.; Ogawa, K.; Araki, Y.; Ito, O.; Kobuke, Y. *Chem.−Eur. J.* **2008**, *14*, 2827–2841. (b) Mateo-Alonso, A.; Ehli, C.; Aminur Rahman, G. M.; Guldi, D. M.; Fioravanti, G.; Marcaccio, M.; Paolucci, F.; Prato, M. *Angew. Chem., Int. Ed.* **2007**, *46*, 3521–3525. (c) Sandanayaka, A. S. D.; Sasabe, H.; Araki, Y.; Furusho, Y.; Ito, O.; Takata, T. *J. Phys. Chem. A* **2004**, *108*, 5145–5155.

(22) (a) Filippone, S.; Barroso, M. I.; Martin-Domenech, A.; Osuna, S.; Sola, M.; Martin, N. *Chem.−Eur. J.* **2008**, *14*, 5198–5206. (b) Lukoyanova, O.; Cardona, C. M.; Aaltable, M.; Filippone, S.; Domenech, A. M.; Martin, N.; Echegoyen, L. *Angew. Chem., Int. Ed.* **2006**, *45*, 7430–7433. (c) Martin, N.; Altable, M.; Filippone, S.; Martin-Domenech, A.; Echegoyen, L.; Cardona, C. M. *Angew. Chem., Int. Ed.* **2006**, *45*, 110–114.

Scheme 1. Synthesis of Triphenylaminofulleropyrrolidine Electron Donor−Acceptor Conjugates

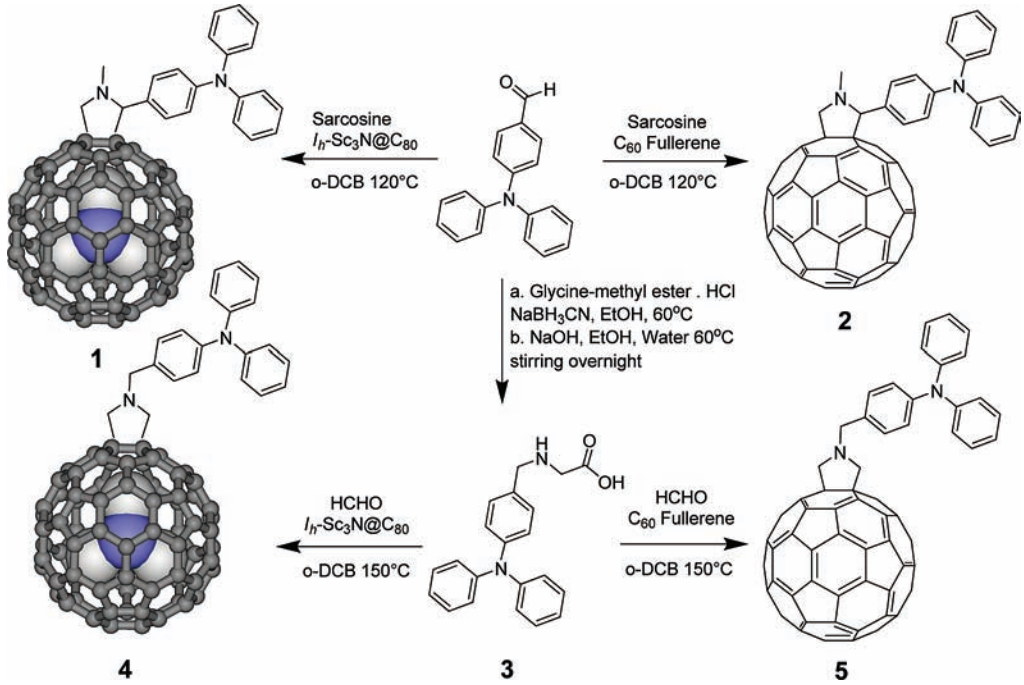

free radical addition.[29] However, the 1,3-dipolar cycloaddition has been the most successful reaction for the functionalization of I_h-$Sc_3N@C_{80}$. The moderate to good yields, the high regioselectivity, and availability or easy preparation of the starting materials make this reaction attractive for the construction of donor−acceptor conjugates. Thus, we decided to pursue this strategy for the synthesis of the TPA-based electron donor−acceptor conjugates as depicted in Scheme 1.

Starting from an isomeric mixture of I_h- and D_{5h}-$Sc_3N@C_{80}$ provided by Luna Innovations Inc., the icosahedral isomer was purified by selective chemical oxidation.[11f] After isolating the I_h-$Sc_3N@C_{80,}$ compound **1** was obtained in a ~40% yield by reacting I_h-$Sc_3N@C_{80}$ with 50 equiv of 4-(*N*-diphenylamino)-benzaldehyde and 15 equiv of sarcosine in *o*-dichlorobenzene (*o*-DCB) at 120 °C. The ^{1}H NMR spectrum obtained in a 4:1 mixture of CS_2/CD_2Cl_2 under selective irradiation of the residual solvent signal shows individual resonances for the protons in the pyrrolidine ring at 4.35, 3.74, and 3.07 ppm (Figure 1a). The 1.28 ppm separation of the resonances for the diastereotopic geminal protons ($J = 9$ Hz) in the pyrrolidine ring, attached to the same carbon atom as inferred by the HMQC spectrum—see Supporting Information—is consistent with the formation of the [5,6]-regioisomer, which is additionally supported by electrochemical studies—see Electrochemical Studies. The protons of the methyl group attached to the nitrogen appear as a singlet at 2.63 ppm. The protons in the aromatic ring directly attached to the pyrrolidine appear as broad signals at 7.92 and 7.38 ppm

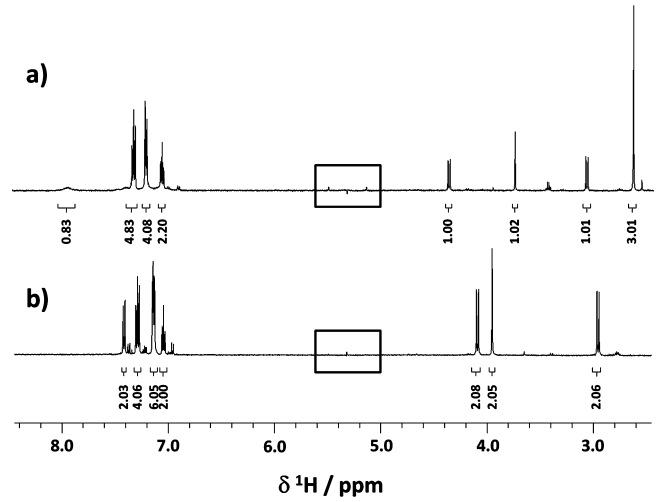

Figure 1. 500 MHz ^{1}H NMR spectrum of (a) compound **1** and (b) compound **4**. Both spectra were obtained using a CS_2/CD_2Cl_2 4:1 mixture as solvent under selective irradiation for suppressing the residual solvent signal as shown within the boxes.

(23) (a) Iezzi, E. B.; Duchamp, J. C.; Harich, K.; Glass, T. E.; Lee, H. M.; Olmstead, M. M.; Balch, A. L.; Dorn, H. C. *J. Am. Chem. Soc.* **2002**, *124*, 524–525. (b) Lee, H. M.; Olmstead, M. M.; Iezzi, E.; Duchamp, J. C.; Dorn, H. C.; Balch, A. L. *J. Am. Chem. Soc.* **2002**, *124*, 3494–3495.

(24) Iezzi, E. B.; Cromer, F.; Stevenson, P.; Dorn, H. C. *Synth. Met.* **2002**, *128*, 289–291.

(25) (a) Cai, T.; Ge, Z.; Iezzi, E. B.; Glass, T. E.; Harich, K.; Gibson, H. W.; Dorn, H. C. *Chem. Commun.* **2005**, 3594–3596. (b) Cardona, C. M.; Kitaygorodskiy, A.; Ortiz, A.; Herranz, M. A.; Echegoyen, L. *J. Org. Chem.* **2005**, *70*, 5092–5097. (c) Cai, T.; Slebodnick, C.; Xu, L.; Harich, K.; Glass, T. E.; Chancellor, C.; Fettinger, J. C.; Olmstead, M. M.; Balch, A. L.; Gibson, H. W.; Dorn, H. C. *J. Am. Chem. Soc.* **2006**, *128*, 6486–6492. (d) Cardona, C. M.; Elliott, B.; Echegoyen, L. *J. Am. Chem. Soc.* **2006**, *128*, 6480–6485. (e) Chen, N.; Fan, L.; Tan, K.; Wu, Y.; Shu, C.; Lu, X.; Wang, C. *J. Phys. Chem. C* **2007**, *111*, 11823–11828.

(26) (a) Wakahara, T.; Iiduka, Y.; Ikenaga, O.; Nakahodo, T.; Sakuraba, A.; Tsuchiya, T.; Maeda, Y.; Kako, M.; Akasaka, T.; Yoza, K.; Horn, E.; Mizorogi, N.; Nagase, S. *J. Am. Chem. Soc.* **2006**, *128*, 9919–9925. (b) Iiduka, Y.; Ikenaga, O.; Sakuraba, A.; Wakahara, T.; Tsuchiya, T.; Maeda, Y.; Nakahodo, T.; Akasaka, T.; Kako, M.; Mizorogi, N.; Nagase, S. *J. Am. Chem. Soc.* **2005**, *127*, 9956–9957.

(27) Shustova, N. B.; Popov, A. A.; Mackey, M. A.; Coumbe, C. E.; Phillips, J. P.; Stevenson, S.; Strauss, S. H.; Boltalina, O. V. *J. Am. Chem. Soc.* **2007**, *129*, 11676–11677.

(28) Shu, C.; Cai, T.; Xu, L.; Zuo, T.; Reid, J.; Harich, K.; Dorn, H. C.; Gibson, H. W. *J. Am. Chem. Soc.* **2007**, *129*, 15710–15717.

(29) Shu, C.; Slebodnick, C.; Xu, L.; Champion, H.; Fuhrer, T.; Cai, T.; Reid, J. E.; Fu, W.; Harich, K.; Dorn, H. C.; Gibson, H. W. *J. Am. Chem. Soc.* **2008**, *130*, 17755–17760.

due to a dynamic effect produced by the restricted rotation of the bulky triphenylamine group.[30]

The same effect is observed in the C_{60} conjugate;[16f] however, the effect is more intense in the I_h-$Sc_3N@C_{80}$ conjugate, which is probably a consequence of the cage size. Increasing the temperature to 40 °C did not change appreciably the appearance of the spectrum. For the remaining aromatic rings, the protons in the ortho position with respect to the nitrogen atom in the TPA group are observed as a doublet centered at 7.18 ppm, the protons in the meta position are observed as a triplet centered at 7.29 ppm and the protons in the para position appear as a triplet centered at 7.03 ppm. These assignments are confirmed by the COSY spectrum—see Supporting Information.

Compound **4** was prepared following a strategy similar to the one used for the preparation of compound **1**. However, paraformaldehyde was added in three portions to the mixture of I_h-$Sc_3N@C_{80}$ and **3** in *o*-DCB within a half hour period to compensate the losses due to the evaporation. A higher temperature was also employed, since the formation of the product **4** was slower when compared to the formation of compound **1**, giving satisfactory yields of the desired product. However, formation of undesired byproducts also increased, which made the purification process harder. Thus, the selected temperature (150 °C) was a compromise between short reaction times and low production of undesirable byproducts.

In the ^{1}H NMR spectrum of compound **4** the pyrrolidine protons appear as two doublets centered at 4.10 and 2.96 ppm, respectively (Figure 1b). A correlation observed in the HMQC spectrum between those signals and a carbon atom at 69.0 ppm indicates the formation of the 5,6-isomer—see Supporting Information. The benzyl protons are observed as a sharp singlet at 3.96 ppm, which correlates with a carbon at 58.5 ppm. The aromatic protons are observed as a group of four signals in the region between 7.0 and 7.5 ppm. The resonances of the ring containing the benzyl group appear at 7.45 and 7.18 ppm, whereas the protons on the remaining aromatic rings are observed at 7.33, 7.18, and 7.08 ppm, respectively. The well-defined ^{1}H NMR signals are evidence that in compound **4** the fullerene does not affect the rotation dynamics of the attached addend as in the case of compound **1**.

Evidence showing the higher thermal stability of compound **4** when compared to that of compound **1** was obtained upon refluxing an *o*-DCB solution containing both compounds in open air and following the retro-cycloaddition process by HPLC (Figure 2). It was observed that the intensity of the peak corresponding to compound **1** decreases faster than that corresponding to compound **4**. It has been proved that the retro Prato reaction strongly depends on the nature of the attached addend.[22a] Therefore, our observations can be explained by the relative thermodynamic stabilities of the corresponding azomethine ylides, which are intermediates during the decomposition process; probably the TPA substituent in the 2-position stabilizes better the corresponding azomethine ylide hence it can leave easily the surface of the fullerene.[22a] The MALDI-TOF mass spectra of compounds **1** and **4** show a strong peak at 1109 *m*/*z* corresponding to I_h-$Sc_3N@C_{80}$ resulting from fragmentation of the parent compounds—see Supporting Information. However, compound **4** shows a much larger relative molecular peak when compared to compound **1**. Even though the fragmentation process depends on many factors, these data seem to confirm the observed trend.

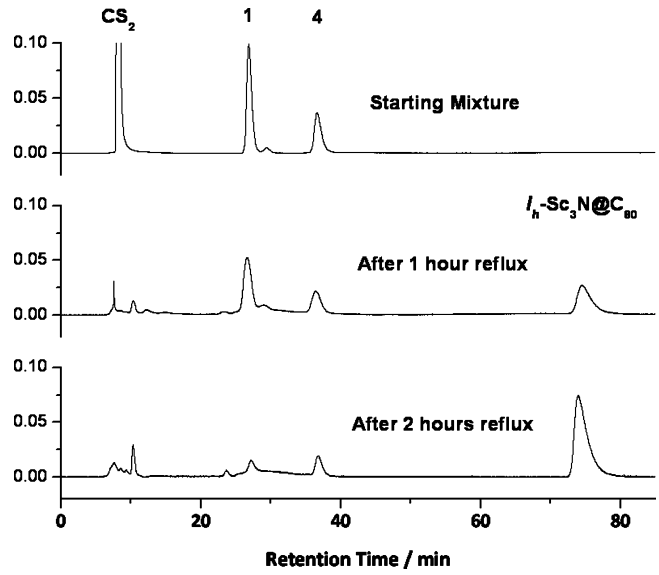

Figure 2. Study of the thermal stability of the TPA−I_h-$Sc_3N@C_{80}$ electron donor−acceptor conjugates **1** and **4**. A solution of compounds **1** and **4** in *o*-DCB was heated under reflux and the retro-cycloaddition reaction was monitored by HPLC. (Buckyprep 10 mm × 250 mm, toluene 2 mL/min).

Electrochemical Studies. The electrochemical properties of the TPA−I_h-$Sc_3N@C_{80}$ electron donor−acceptor conjugates **1** and **4** were studied by cyclic voltammetry in *o*-DCB using a glassy carbon electrode and a 0.05 M solution of tetra(*n*-butyl)ammonium hexafluorophosphate as supporting electrolyte. The redox couple ferrocene/ferrocenium (Fc/Fc^+) was used as internal standard for referencing the potentials. All the redox potentials for compounds **1**, **2**, **4**, and **5** along with I_h-$Sc_3N@C_{80}$, C_{60} and 4-(diphenylamino)benzyl alcohol used as references are collected in Table 1.

As shown in Figure 3 trace b, **1** exhibits three reversible reductions, which are characteristic for [5,6]-I_h-$M_3N@C_{80}$ fulleropyrrolidine adducts.[13] In the anodic scan **1** exhibits two irreversible oxidation processes. The first oxidation potential occurring at +0.39 V is probably centered on the TPA moiety. The second oxidation potential at +1.06 can be attributed to the oxidation of the pyrrolidine group, based on previous observations.[22b]

Compound **4** has a similar reductive behavior to that of **1**, three reversible reductions based on the I_h-$Sc_3N@C_{80}$ cage. There is also a small wave around −2.0 V that correlates with the irreversible formation of a film over the electrode. This behavior is currently under study in our laboratories. In the anodic scan, **4** has three irreversible oxidations; the process occurring at +0.32 V was assigned to the oxidation of the TPA moiety. The second oxidation occurring at +0.63 V was assigned to the pyrrolidine group and the third at +0.99 V was assigned to the oxidation of the I_h-$Sc_3N@C_{80}$ cage. The first reduction potential is shifted by 50 mV toward positive potentials relative to that for the pristine I_h-$Sc_3N@C_{80}$, while the TPA oxidation potential is shifted toward more negative potentials, which is probably indicative of an electronic interaction between the TPA and the I_h-$Sc_3N@C_{80}$ moieties in the ground state.

Photophysical Studies. Insight into charge transfer interactions within the TPA-fullerene conjugates came from transient absorption measurements, in which the lead compounds, that is, TPA-C_{60} (**2** and **5**) and TPA-I_h-$Sc_3N@C_{80}$ (**1** and **4**) were

(30) Ajamaa, F.; Duarte, T. M. F.; Bourgogne, C.; Holler, M.; Fowler, P. W.; Nierengarten, J. *Eur. J. Org. Chem.* **2005**, 3766–3774.

Table 1. Reduction Potentials in V vs Fc/Fc^{+a}

compound	$E^{2+/3+}$	$E^{+/2+}$	$E^{0/+}$	$E^{0/-}$	$E^{-/2-}$	$E^{2-/3-}$
C_{60}	−	−	−	−1.10(60)	−1.47(60)	−1.91(64)
I_h-$Sc_3N@C_{80}$	−	+1.09[b]	+0.59[b]	−1.26[b]	−1.62[b]	−2.37[b]
1	−	+1.06[b]	+0.39[b]	−1.10(90)	−1.50(88)	−2.23(81)
2	−	−	+0.56(60)	−1.22(64)	−1.60(60)	−2.11(66)
4-(diphenylamino)benzyl alcohol	−	−	+0.51[b]	−	−	−
4	+0.99[b]	+0.63[b]	+0.32[b]	−1.21(86)	−1.59(82)	−2.29(91)
5	−	−	+0.55[b]	−1.18(90)	−1.55(87)	−2.07(81)

[a] All the CVs were recorded in a 0.05 M solution of n-Bu_4NPF_6 in o-DCB. (Glassy carbon working electrode). [b] Irreversible process (reported values are peak potentials).

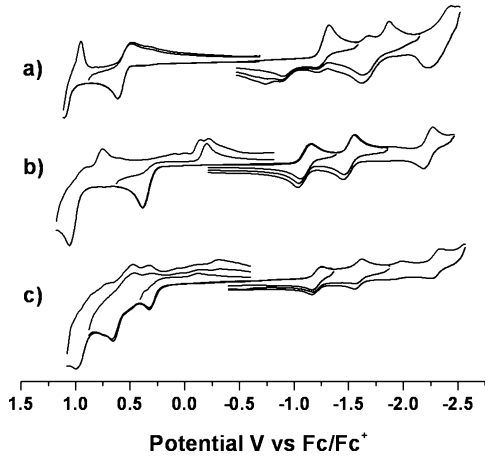

Figure 3. Cyclic voltammograms recorded on a GC electrode (1 mm) in a 0.05 M solution of tetra(*n*-butyl)ammoniumhexafluorophosphate in *o*-DCB as supporting electrolyte and a scan rate of 100 mV/s. (a) Pristine I_h-$Sc_3N@C_{80}$, (b) compound **1**, and (c) compound **4**.

probed in solvents of different polarity (i.e., toluene, carbon disulfide, THF, and benzonitrile). In particular, short excitation at 387 nm afforded the selective excitation of either C_{60} or I_h-$Sc_3N@C_{80}$, whose singlet excited-state characteristics and lifetimes are well documented.[9b,31]

In line with reference experiments we monitored the singlet excited-state characteristics of C_{60}—in **2** and **5**—and of I_h-$Sc_3N@C_{80}$—in **1** and **4**—at 880 and 550/1040 nm, respectively. In contrast to what has been seen for the reference compounds, the C_{60} and I_h-$Sc_3N@C_{80}$ singlet excited-state features decay rather rapidly (∼1.5 ns and ∼100 ps, respectively). Inspecting the transient changes that develop concomitantly with these decays, no spectral resemblance with any known excited state (i.e., C_{60} triplet, I_h-$Sc_3N@C_{80}$ triplet, TPA triplet, etc.)[9b,31] could be established—see Figures 4 and 5. Instead, transient maxima at 610 and 1020 nm suggest charge transfer activity for photoexcited **2** and **5** in THF ($\varepsilon = 7.6$) and benzonitrile ($\varepsilon = 24.8$).

These features resemble the fingerprints of the one-electron oxidized TPA radical cation and the one-electron reduced C_{60} radical anion, respectively.[32] As a matter of fact, our experiments corroborate the successful formation of $TPA^{\bullet+}$-$C_{60}^{\bullet-}$ with rate constants of $7.6 \pm 1.0 \times 10^{10}$ (**2**) and $4.1 \pm 0.5 \times 10^{10}$ s^{-1} (**5**) in THF.

Turning to **1** and **4**, the near-infrared region is, once again, decisive for assigning the radical ion pair state. In line with a previous investigation that focused on the photophysical, radiolytical and spectroelectrochemical generation of one-electron reduced I_h-$Sc_3N@C_{80}$ radical anions a transient maximum at 1060 nm confirms the reduction of this moiety in **1** and **4**.[9a] Formation of the $TPA^{\bullet+}$-I_h-$Sc_3N@C_{80}^{\bullet-}$ radical ion pair state was confirmed by detecting the 610 nm signature of $TPA^{\bullet+}$. The corresponding rate constants were $3.4 \pm 0.5 \times 10^{10}$ and $1.9 \pm 0.5 \times 10^{10}$ s^{-1} for **1** and **4**, respectively, in THF.

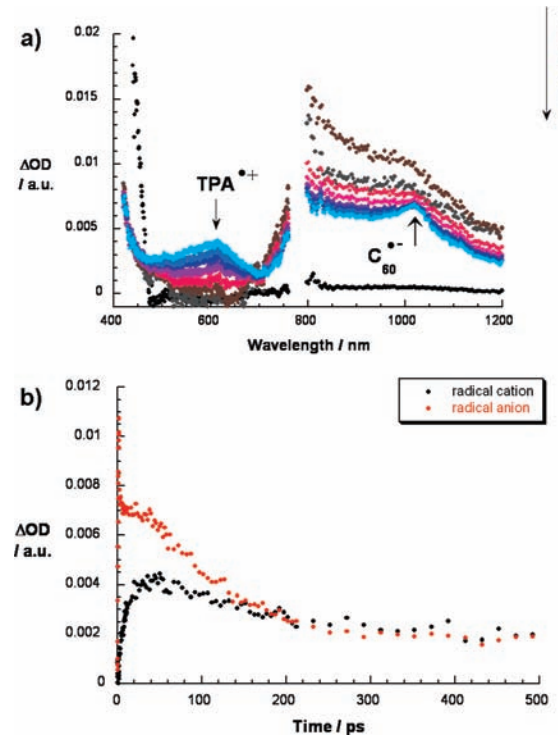

Figure 4. (a) Differential absorption spectra (visible and near-infrared) obtained upon femtosecond flash photolysis (388 nm) of (10^{-5} M) **2** in benzonitrile with several time delays between 0 and 25 ps at room temperature—see legend for time evolution. (b) Time−absorption profile of the spectra shown above at 610 nm (black spectrum) and 1020 nm (red spectrum), reflecting the charge separation and charge recombination dynamics.

In less polar solvents, on the other hand, such as toluene ($\varepsilon = 2.4$) or carbon disulfide ($\varepsilon = 2.6$) the singlet excited-state features of C_{60} or I_h-$Sc_3N@C_{80}$ undergo conventional intersystem crossing—see Figures 6 and 7. They yield the corresponding triplet excited states (C_{60}, 700 nm maximum; I_h-$Sc_3N@C_{80}$, 520 nm maximum) without, however, revealing any significant radical ion pair state formation.

The lack of charge transfer in non-polar solvents was further supported by steady-state fluorescence measurements. As Figure 8 illustrates, in toluene and carbon disulfide the C_{60} and I_h-$Sc_3N@C_{80}$ centered fluorescence is in **1**, **2**, **4**, and **5** unchanged

(31) Guldi, D. M.; Prato, M. *Acc. Chem. Res.* **2000**, *33*, 695–703.
(32) (a) Guldi, D. M.; Asmus, K. D. *J. Phys. Chem. A* **1997**, *101*, 1472–1481. (b) Guldi, D. M. *J. Phys. Chem. A* **1997**, *101*, 3895–3900. (c) Heckmann, A.; Lambert, C. *J. Am. Chem. Soc.* **2007**, *129*, 5515–5527. (d) El-Khouly, M. E.; Shim, S. H.; Araki, Y.; Ito, O.; Kay, K. Y. *J. Phys. Chem. B* **2008**, *112*, 3910–3917.

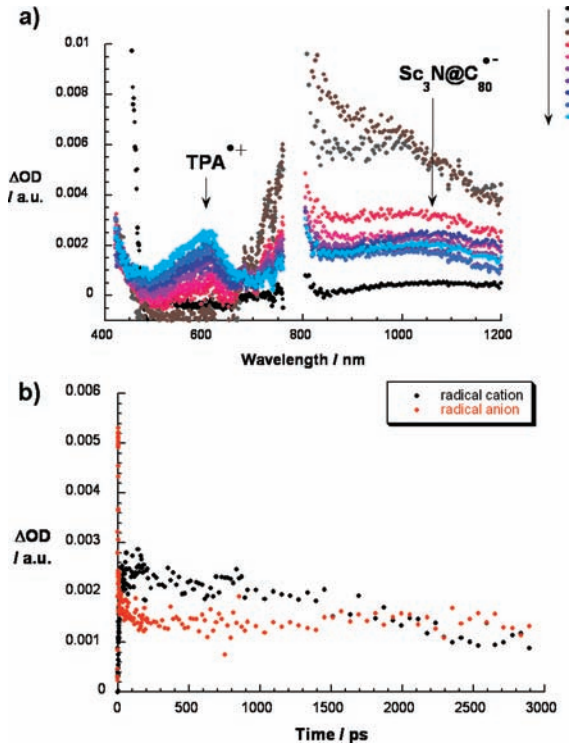

Figure 5. (a) Differential absorption spectra (visible and near-infrared) obtained upon femtosecond flash photolysis (388 nm) of (10^{-5} M) **1** in benzonitrile with several time delays between 0 and 50 ps at room temperature—see legend for time evolution. (b) Time–absorption profile of the spectra shown above at 610 nm (black spectrum) and 1060 nm (red spectrum), reflecting the charge separation and charge recombination dynamics.

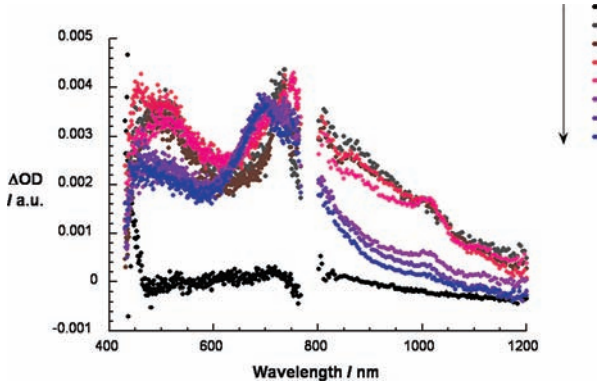

Figure 6. Differential absorption spectra (visible and near-infrared) obtained upon femtosecond flash photolysis (388 nm) (10^{-5} M) of **2** in toluene with several time delays between 0 and 3000 ps at room temperature—see legend for time evolution—reflecting the intersystem crossing dynamics.

relative to the corresponding references. Quantum yields are on the order of 6.0×10^{-4} (**2** and **5**) and 5.3×10^{-5} (**1** and **4**) and, thus, identical to those of the reference systems lacking the electron donor. Notable in toluene and carbon disulfide the energies of the radical ion pair states are higher than those of the singlet excited states. Taking, for example, **2** and **5** we

(33) (a) Weller, A. *Z. Phys. Chem.* **1982**, *133*, 93–98. (b) Imahori, H.; Hagiwara, K.; Aoki, M.; Akiyama, T.; Taniguchi, S.; Okada, T.; Shirakawa, M.; Sakata, Y. *J. Am. Chem. Soc.* **1996**, *118*, 11771–11782. (c) van Dijk, S. I.; Groen, C. P.; Hartl, F.; Brouwer, A.; Verhoeven, J. W. *J. Am. Chem. Soc.* **1996**, *118*, 8425–8432. (d) Hauke, F.; Hirsch, A.; Liu, S. G.; Echegoyen, L.; Swartz, A.; Luo, C.; Guldi, D. M. *Chem. Phys. Chem.* **2002**, *3*, 195–205.

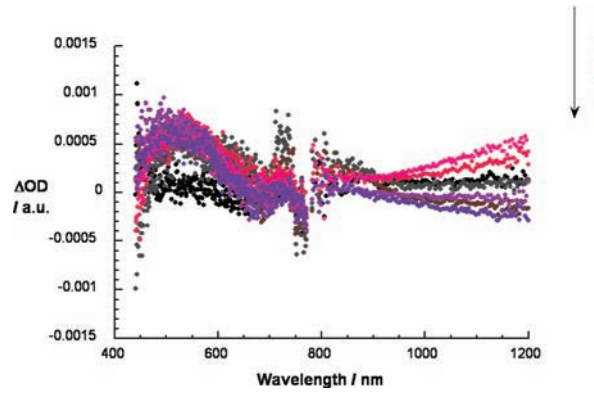

Figure 7. Differential absorption spectra (visible and near-infrared) obtained upon femtosecond flash photolysis (388 nm) of (10^{-5} M) **1** in toluene with several time delays between 0 and 3000 ps at room temperature—see legend for time evolution—reflecting the intersystem crossing dynamics.

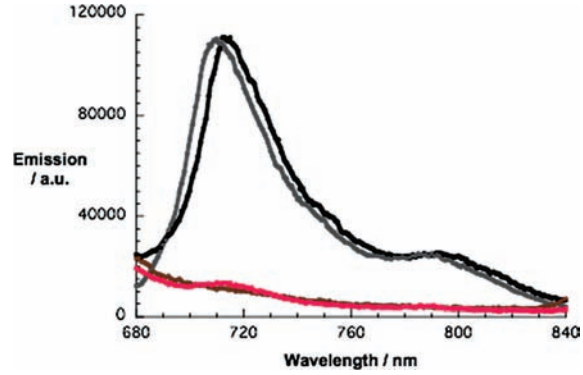

Figure 8. Room temperature fluorescence spectra of **2** in toluene (i.e., black spectrum), carbon disulfide (i.e., gray spectrum), THF (i.e., brown spectrum), and benzonitrile (i.e., red spectrum) exhibiting the same optical absorption of 0.05 at the 355 nm excitation wavelength.

calculate—via the Dielectric Continuum model[33]—energies of around 2.37 and 2.42 eV in toluene and carbon disulfide, respectively, while that of the C_{60} singlet excited state is around 1.76 eV.

Similarly, the I_h-$Sc_3N@C_{80}$ singlet excited state is 1.5 eV below the radical ion pair state of **1** and **4** in toluene and carbon disulfide (i.e., 1.9 and 2.0 eV). These thermodynamic considerations suggest that a competitive scenario, namely intersystem crossing versus charge separation is unlikely to play a role in toluene and carbon disulfide. Any radical ion pair state should be generated only as a minor product. THF and benzonitrile revealed, on the other hand, quenching of at least a factor greater than 50 with radical ion pair state energies of 1.67 eV in THF and 1.45 eV in benzonitrile (**2** and **5**), as well as 1.42 eV in THF and 1.22 eV in benzonitrile (**1** and **4**). Please compare these values to the singlet excited-state energies of **2**/**5** (1.76 eV) and **1**/**4** (1.5 eV).

Important is the comparison of rate constants (i.e., charge separation and charge recombination) for **2** and **5** versus **1** and **4**, which should shed light onto the stabilization of the radical ion pair states when employing I_h-$Sc_3N@C_{80}$ as a novel electron accepting building block. The fingerprints of $TPA^{\bullet+}$-$C_{60}^{\bullet-}$ and $TPA^{\bullet+}$-I_h-$Sc_3N@C_{80}^{\bullet-}$ proved to be valuable assets to fit the growth and decay dynamics of the radical cation and radical anion species.

When turning to charge separation—located evidently in the normal region of the Marcus parabola—lower singlet excited-

Table 2. Rate Constants and Thermodynamic Driving Forces for Charge Transfer in **1**, **2**, **4**, and **5**

compound	k_{CS}/THF[s^{-1}]	$-\Delta G_{CS}$/THF[eV]	k_{CR}/THF[s^{-1}]	k_{CR}/bzcn[s^{-1}]	$-\Delta G_{CR}$/THF[eV]	$-\Delta G_{CR}$/bzcn[eV]
compound **1**	$3.4 \pm 0.5 \times 10^{10}$	0.08	$1.7 \pm 0.5 \times 10^{9}$	$4.5 \pm 0.5 \times 10^{8}$	1.42	1.22
compound **2**	$7.6 \pm 1.0 \times 10^{10}$	0.09	$8.0 \pm 1.0 \times 10^{9}$	$6.5 \pm 0.5 \times 10^{9}$	1.67	1.45
compound **4**	$1.9 \pm 0.5 \times 10^{10}$	0.08		$<3.3 \pm 0.5 \times 10^{8}$	1.42	1.22
compound **5**	$4.1 \pm 0.5 \times 10^{10}$	0.09		$1.9 \pm 0.5 \times 10^{9}$	1.67	1.45

state energies in **1/4** when compared to **2/5** are nearly compensated by lower radical ion pair state energies. In fact, the driving forces for charge separation are nearly identical in THF (0.08 eV in **1/4** vs 0.09 eV in **2/5**) and benzonitrile (0.28 eV in **1/4** vs 0.31 eV in **2/5**). In line with this thermodynamic consideration, **2** and **5** tend to charge separate only slightly faster with rate constants of around 6×10^{10} s^{-1} in THF and benzonitrile than **1** and **4**, for which rate constants of around 5×10^{10} s^{-1} were determined. Increasing the donor−acceptor separation, which was accomplished by linking TPA to the nitrogen of the pyrrolidine ring rather than to the carbon of the pyrrolidine ring exerts a profound impact on the charge separation dynamics, namely a notable slow down. For the charge recombination processes, a "stabilizing" trend is unambiguously given, when considering the corresponding rate constants of $6.5 \pm 0.5 \times 10^{9}$ (**2**), $1.9 \pm 0.5 \times 10^{9}$ (**5**), $4.5 \pm 0.5 \times 10^{8}$ (**1**), and $<3.3 \pm 0.5 \times 10^{8}$ s^{-1} (**4**) in benzonitrile. A similar stabilization evolves in THF with rate constants of $8.0 \pm 1.0 \times 10^{9}$ and $1.7 \pm 0.5 \times 10^{9}$ s^{-1} for **2** and **1**, respectively. Nevertheless, we note a relationship—rate constant vs solvent polarity (see Table 2)—that suggests dynamics in the normal region of the Marcus parabola, where the rate constants increase with increasing thermodynamic driving force ($-\Delta G°$).[34] In this light, the stabilization seen for **1** and **4**—relative to **2** and **5**—is rationalized on smaller driving forces.

Conclusions

We have synthesized two isomeric triphenylamine−I_h-$Sc_3N@C_{80}$ derivatives by 1,3-dipolar cycloaddition reactions. The compound with the *N*-connected donor has significantly better thermal stability and longer lived photoinduced charge separated state than the corresponding 2-substituted system. The I_h-$Sc_3N@C_{80}$ dyads have considerably longer lived photoinduced charge separated states and lower first reduction potentials than their C_{60} analogues, confirming the advantage of using I_h-$Sc_3N@C_{80}$ for replacing C_{60} as the acceptor moiety for the construction of donor−acceptor conjugates.

Experimental Section

Materials and Methods. The isomeric mixture of I_h- and D_{5h}-$Sc_3N@C_{80}$ was provided by Luna Innovations (Nanoworks division). Pure I_h-$Sc_3N@C_{80}$ was obtained by eluting a solution of the isomeric mixture through a plug of silica gel containing "Magic Blue" (tris(4-bromophenyl)aminiumhexachloroantimonate), which selectively oxidized the D_{5h} isomer. All reactions were run under an argon atmosphere and followed by TLC on silica plates. Anhydrous and deuterated solvents were purchased from Aldrich and used as received. NMR spectra were obtained using Bruker Avance 500 spectrometer using TMS or residual solvent signals as internal reference. MALDI-TOF mass spectra were obtained on a Voyager-DE STR mass spectrometer. HPLC was performed using a Varian Prostar 210 equipped with a Buckyprep column (10 mm × 250 mm). All electrochemical measurements were performed in *o*-DCB with 0.05 mol dm^{-3} tetra(*n*-butyl)ammonium hexafluorophosphate (n-Bu_4NPF_6) as supporting electrolyte. Voltammetric experiments were performed using a potentiostat/galvanostat Model CHI660A (CH Instruments electrochemical workstation) with a three-electrode cell placed in a Faraday cage. The working electrode consisted of a glassy carbon disk (Bioanalytical Systems, Inc.) with a diameter of 1 mm. The surface of the electrode was polished using 0.25 μm diamond polishing compound (Metadi II, Buehler). The electrode was then sonicated in water in order to remove traces of alumina from the metal surface, washed with water, and dried. A silver wire was used as a pseudoreference electrode. All the potentials were calibrated against the ferrocene/ferrocenium (Fc/Fc^+) redox couple. A platinum wire was used as counter electrode; it was cleaned by heating in a flame for ~30 s. The solution was deaerated for 20 min with argon prior to the electrochemical measurements. Femtosecond transient absorption studies were performed with 387 nm laser pulses (1 kHz, 150 fs pulse width) from an amplified Ti:Sapphire laser system (Model CPA 2101, Clark-MXR Inc.). Emission spectra were recorded with a Fluoromax 3 (Horiba) spectrofluorometer. The experiments were performed at room temperature. Each spectrum represents an average of at least five individual scans, and appropriate corrections were applied whenever necessary.

***N*-Methyl-2-(4-diphenylaminophenyl)-[5,6]-I_h-$Sc_3N@C_{80}$-fulleropyrrolidine (1).** I_h-$Sc_3N@C_{80}$ (9.82 mg, 8.85 μmol, 1 equiv) was poured in a 100 mL Schlenk flask along with 121.80 mg of 4-(diphenylamino)benzaldehyde (445 μmol, 50 equiv) and 11.48 mg of sarcosine (128.85 μmol, 14.5 equiv). The solids were dissolved in 50 mL *o*-DCB and heated to 120 °C under argon for 90 min. The solvent was finally removed under high vacuum. The remaining solid was then dissolved in CS_2 and purified on a silica gel column eluting first with CS_2 for removing the unreacted I_h-$Sc_3N@C_{80}$ followed by a 1:1 mixture of CS_2 and toluene for eluting the product. After evaporating the solvent and washing with ethyl ether 5.15 mg of product was obtained. Yield 40.6%; 41.2% subtracting the recovered I_h-$Sc_3N@C_{80}$. This compound has retention time 26.73 min in Buckyprep column (10 × 250 mm), toluene 2 mL/min. ^{1}H NMR (CS_2/CD_2Cl_2 4:1, 500 MHz, δ) 7.92 broad (s, 2H), 7.38 broad (s, 2H), 7.30 (pseudo-t, 4H, J 7.5 Hz), 7.18 (d, 4H, J 7.5 Hz), 7.04 (t, 2H, J 7.5 Hz), 4.35 (d, 1H, J 9 Hz), 3.74 (s, 1H), 3.07 (d, 1H, J 9 Hz), 2.63 (s, 3H). MALDI *m/z* 1411.97 (negative ionization, 9-nitroanthracene as matrix). Following the same procedure but using C_{60} (25.24 mg, 35 μmol, 1 equiv), sarcosine (9.4 mg, 105 μmol, 3 equiv) and 4-(diphenylamino)benzaldehyde (95.9 mg, 350 μmol, 10 equiv). Compound **2** was obtained with a 40% yield (15.7 mg, 14 μmol) after purification. Its NMR data matches completely the previous reported values.[17f]

***N*-(Benzyl-4-diphenylaminophenyl)glycine (3).** 4-(Diphenylamino)benzaldehyde (352.0 mg, 1.29 mmol, 1 equiv) and glycine methyl ester hydrochloride (326.0 mg, 2.59 mmol, 2 equiv) were poured in a 200 mL Schlenk flask equipped with a stirring bar under argon. Anhydrous ethanol (100 mL) was added, the stirring started and the mixture heated to 60 °C. Once the starting materials were dissolved the solution turned to a yellowish color. At that point dropwise addition of $NaBH_3CN$ (0.705 g, 11.2 mmol, 3 equiv) suspended in anhydrous ethanol was started and continued for a period of 3 h. Finally the solvent was removed under vacuum and the residual solid treated with 5% HCl solution for destroying the excess of $NaBH_3CN$. A saturated $NaHCO_3$ solution was added dropwise until a neutral pH was reached. The whole mixture was extracted with CH_2Cl_2 and dried with anhydrous Na_2SO_4, and the solution filtered through a silica plug. After evaporating the solvent the intermediate ester was obtained and used in the next step without

(34) Marcus, R. A. *J. Chem. Phys.* **1956**, *24*, 966–978.

further purification. ^{1}H NMR (CD_2Cl_2, 500 MHz, δ) 7.34−7.28 (m, 6H), 7.16−7.04 (m, 8H), 3.84 (s, 2H), 3.78 (s, 3H), 3.51 (s, 2H). ^{13}C NMR (CD_2Cl_2, 125 MHz, δ) 172.6 carbonyl, 147.9 q, 146.9 q, 134.1 q, 129.3 CH, 129.2 CH, 124.2 CH, 124.1 CH, 122.7 CH, 52.5 φ-CH_2−N, 51.6 −O−CH_3, and 49.7 N−CH_2COO. This compound was dissolved in 20 mL of ethanol/water 8:1 and a 0.20 mL of saturated NaOH solution was added. The whole mixture was heated to 50 °C and stirred overnight. The final reaction mixture was cooled and HCl 5% added dropwise until a neutral pH was reached, which crashes the product out of the solution. The white solid obtained was washed with cold deionized water and dried under vacuum. Finally 98.5 mg of product was obtained (23% yield). ^{1}H NMR (DMSO, 500 MHz, δ) 9.57 broad (s, 1H), 7.42 (d, 2H, J 9 Hz), 7.32 (t, 4H, J 7.5 Hz), 7.08 (t, 2H, J 7.5 Hz), 7.02 (d, 4H, J 7.5 Hz), 6.97 (d, 2H, J 9 Hz), 4.08 (s, 2H), 3.81 (s, 2H). ^{13}C NMR (DMSO, 125 MHz, δ) 167.8 carbonyl, 148.0 q, 146.9 q, 131.6 CH, 129.6 CH, 125.0 q, 124.3 CH, 123.5 CH, 122.5 CH, 49.3 φ-CH_2−N, 46.1 N−CH_2COO.

***N*-(Benzyl-4-diphenylaminophenyl)-[5,6]-I_h-$Sc_3N@C_{80}$-fulleropyrrolidine (4).** I_h-$Sc_3N@C_{80}$ (12.1 mg, 10.9 μmol, 1 equiv) was poured in a 100 mL Schlenk flask along with **3** (34.5 mg, 109.1 μmol, 10 equiv), and 40 mL of anhydrous *o*-DCB was added by using a cannula. This mixture was heated to 150 °C under argon and slurry made with paraformaldehyde (24.5 mg, 816 μmol, 75 equiv) in 10 mL of anhydrous *o*-DCB was added in three portions every 15 min; heating was continued while following the reaction by TLC on silica plates eluting with CS_2/toluene 2:1. The reaction was stopped when the formation of bis-adducts and poly adducts was observed in the TLC plates even though the starting I_h-$Sc_3N@C_{80}$ had not been consumed completely. The solvent was then removed under high vacuum and the remaining solid dissolved in CS_2 and purified on a silica gel column eluting first with CS_2 for removing the unreacted I_h-$Sc_3N@C_{80}$ followed by a 1:1 mixture of CS_2 and toluene for eluting the product. After evaporating the solvent and washing with ethyl ether 5.50 mg of product was obtained. Yield 38.5%; 43.8% subtracting the recovered I_h-$Sc_3N@C_{80}$. This compound has retention time 37.3 min in Buckyprep column (10 mm × 250 mm), toluene 2 mL/min. ^{1}H NMR (CS_2/CD_2Cl_2 4:1, 500 MHz, δ) 7.46 (d, 2H, J 8.5 Hz), 7.33 (pseudo-t, 4H, J 7.5 Hz), 7.20−7.15 (m, 6H), 7.09 (t, 2H, J 7.5 Hz), 4.13 (d, 2H, J 10 Hz), 3.99 (s, 2H), 2.99 (d, 2H, J 10 Hz). MALDI *m*/*z* 1411.68 (negative ionization, 9-nitroanthracene as matrix). Following the same procedure but using C_{60} (23.2 mg, 32.2 μmol, 1 equiv), **3** (30.2 mg, 95.5 μmol, 3 equiv), and paraformaldehyde (24.0 mg, 800 μmol, 25 equiv). Compound **5** was obtained with a 32% yield (10.6 mg, 10.3 μmol) after purification. ^{1}H NMR (CS_2/CD_2Cl_2 2:1, 500 MHz, δ) 7.58 (d, 2H, J 8.5 Hz), 7.27 (t, 4H, J 7.5 Hz), 7.16 (d, 2H, 8.5 Hz), 7.12 (d, 4H, J 7.5 Hz), 7.02 (t, 2H, J 7.5 Hz), 4.50 (s, 4H), 4.28 (s, 2H). ^{13}C NMR (CS_2/CD_2Cl_2 2:1, 125 MHz, δ) 155.14 q, 147.79 q, 147.40 q, 147.33 q, 146.37 q, 146.24 q, 146.18 q, 145.82 q, 145.59 q, 145.40 q, 144.69 q, 143.23 q, 142.76 q, 142.39 q, 142.21 q, 142.03 q, 140.32 q, 136.45 q, 132.21 q, 129.84 CH, 129.48 CH, 124.48 CH, 124.08 CH, 123.08 CH, 70.86 q, 67.83 Bz−N−$(CH_2)_2$, 58.67 φ-CH_2−N. MALDI *m*/*z* 1020.47 (positive ionization, 9-nitroanthracene as matrix).

Acknowledgment. We are grateful to Luna Innovations Inc. for providing us with the initial mixture of fullerenes. We also thank the National Science Foundation (Grant No. DMR 0809129 to L.E.) for support and J. Walls for assistance. This material was also based upon work supported by Luna Innovations Inc. and the Air Force Office of Scientific Research (AFOSR) under Contract No. FA9550-06-C-0010. G.B. thanks the Spanish MEC for a "Ramón y Cajal" contract. The Voyager-DE STR mass spectrometer was purchased in part with a grant from the Division of Research Resources, National Institutes of Health (RR 11966). Also the Deutsche Forschungsgemeinschaft (SFB 583), FCI and Office of Basic Energy Sciences of the U.S. Department of Energy are gratefully acknowledged. S.S.G. gratefully acknowledges the support from Alexander von Humboldt Foundation. This paper is dedicated to Professor Fritz Wasgestion on the occasion of his 75th birthday.

Supporting Information Available: HPLC traces, CVs, MALDI-TOF mass spectra, and 2D-NMR spectroscopy data for all the new compounds. This material is available free of charge via the Internet at http://pubs.acs.org.

JA900612G